Theoretical and Applied Genetics
https://doi.org/10.1007/s00122-019-03288-2

ORIGINAL ARTICLE

A major QTL co-localized on chromosome 6BL and its epistatic interaction for enhanced wheat stripe rust resistance

Qingdong Zeng[1] · Jianhui Wu[1] · Shengjie Liu[1,2] · Shuo Huang[1,2] · Qilin Wang[1] · Jingmei Mu[1,2] · Shizhou Yu[1,2] · Dejun Han[1,2] · Zhensheng Kang[1,3]

Received: 22 September 2018 / Accepted: 16 January 2019

Abstract

Key message **Co-localization of a major QTL for wheat stripe rust resistance to a 3.9-cM interval on chromosome 6BL across both populations and another QTL on chromosome 2B with epistatic interaction.**

Abstract Cultivars with diverse resistance are the optimal strategy to minimize yield losses caused by wheat stripe rust (*Puccinia striiformis* f. sp. *tritici*). Two wheat populations involving resistant wheat lines P10078 and Snb"S" from CIMMYT were evaluated for stripe rust response in multiple environments. Pool analysis by Wheat660K SNP array showed that the overlapping interval on chromosome 6B likely harbored a major QTL between two populations. Then, linkage maps were constructed using KASP markers, and a co-localized locus with large effect on chromosome 6BL was detected using QTL analysis in both populations. The coincident QTL, named *QYr.nwafu-6BL.2*, explained 59.7% of the phenotypic maximum variation in the Mingxian 169 × P10078 and 52.5% in the Zhengmai 9023 × Snb"S" populations, respectively. This co-localization interval spanning 3.9 cM corresponds to ~ 30.5-Mb genomic region of the newest common wheat reference genome (IWGSC RefSeq v.1.0). In addition, another QTL was also detected on chromosome 2B in Zhengmai 9023 × Snb"S" population and it can accelerate expression of *QYr.nwafu-6BL.2* to enhance resistance with epistatic interaction. Allowing for *Pst* response, marker genotypes, pedigree analysis and relative genetic distance, *QYr.nwafu-6BL.2* is likely to be a distinct adult plant resistance QTL. Haplotype analysis of *QYr.nwafu-6BL.2* revealed specific SNPs or alleles in the target region from a diversity panel of 176 unrelated wheat accessions. This QTL region provides opportunity for further map-based cloning, and haplotypes analysis enables pyramiding favorable alleles into commercial cultivars by marker-assisted selection.

Introduction

Wheat production must increase more rapidly and at a higher rate than in the past to satisfy demand of the world's growing population as a staple foodstuff (Ray et al. 2012). However, changes in climate patterns across environments along with multiple biotic and abiotic stresses present a huge challenge for continuing yield stability (Abberton et al. 2016; Brummer et al. 2011). The rusts, especially stripe rust or yellow rust (YR) caused by *Puccinia striiformis* Westend. f. sp. *tritici* Erikss. (*Pst*), are among the most serious threats (Hovmøller et al. 2010; McIntosh et al. 1995). With a total annual wheat planting area of about 22 million hectares (http://www.stats.gov.cn/), China is the largest producer as well as the largest stripe rust epidemic region in the world (Stubbs 1985). Stripe rust occurs periodically in almost all winter wheat-growing regions of China, and several major epidemics have caused losses amounting to several million metric tons of grain (Chen et al. 2009; Li and Zeng 2002;

Communicated by Hermann Buerstmayr.

Qingdong Zeng, Jianhui Wu and Shengjie Liu have contributed equally to this work.

Electronic supplementary material The online version of this article (https://doi.org/10.1007/s00122-019-03288-2) contains supplementary material, which is available to authorized users.

✉ Dejun Han
handj@nwsuaf.edu.cn

✉ Zhensheng Kang
kangzs@nwsuaf.edu.cn

[1] State Key Laboratory of Crop Stress Biology for Arid Areas, Northwest A&F University, Yangling 712100, Shaanxi, People's Republic of China

[2] College of Agronomy, Northwest A&F University, Yangling 712100, Shaanxi, People's Republic of China

[3] College of Plant Protection, Northwest A&F University, Yangling 712100, Shaanxi, People's Republic of China

Published online: 01 February 2019

Wan et al. 2004). The most serious cause is the evolution of new pathotypes or races with virulence for currently widely deployed resistance genes (Chen and Kang 2017; Tang et al. 2018).

Fungicide control is often effective, but it increases the cost of production and may have hidden environmental problems (Chen 2014). On the contrary, stacking effective resistance (*R*) genes in commercial cultivars is the most reliable control strategy. Unfortunately, most of the characterized all-stage resistance (ASR) genes are no longer effective against current *Pst* race groups in China (Sharma-Poudyal et al. 2013; Wu et al. 2018c; Zeng et al. 2015). Adult plant resistance (APR), or high-temperature adult plant resistance (HTAPR), genes have been utilized by many breeding programs worldwide as some of these genes have remained effective for long time periods (Chen 2013). It indicates that some APR genes are not race specific—that is why they have remained durable. Other APR genes (*Yr11*, *Yr12*, *Yr13* and *Yr14*) are race specific and not durable (Hovmøller 2007). Although a single APR/HTAPR gene might not provide adequate protection against loss, stacking such genes usually enhances the level and stability of protection (Ellis et al. 2014). Moreover, the broad-spectrum virulence of current races is forcing breeders to identify and utilize more APR genes to accelerate the resistance breeding effort in doing so.

Conventional gene/QTL mapping is a time-consuming, laborious and costly process (Xu and Crouch 2008). Especially for common wheat, the hexaploid nature hinders application and development of genomics tools for crop improvement (Uauy 2017). It is therefore an onerous task to identify polymorphic markers in this species. Traditional molecular markers are always polymerase chain reaction (PCR) markers based on sequence fragment polymorphisms. They are often low density, low throughput, somewhat difficult to use, and have no correlation with functional genes or alleles (Wang et al. 2015). The advent of next-generation sequencing (NGS) technologies has radically changed the landscape. NGS enables efficient high-throughput discovery of DNA variants, and new generation markers in the form of single nucleotide polymorphisms (SNP) provide high resolution of genetic diversity (Wang et al. 2018). Different genotyping platforms with high densities of markers and considerable flexibility such as Illumina Bead Array™, Affymetrix Gene Chip™ and kompetitive allele specific PCR (KASP) have become available for genetic studies and breeding purposes (Rasheed et al. 2017). Bulked segregant analysis (BSA), or pooled analysis (Giovannoni et al. 1991; Michelmore et al. 1991), involving selected and pooled DNA samples from contrasting phenotypic pools, provides a simple and rapid initial approach in searching for DNA variants linked to specific genomic regions conferring a trait of interest. The combination of BSA and high-throughput genotyping technology is a powerful tool for accelerating gene identification and QTL mapping (Schlötterer et al. 2014; Wu et al. 2018d; Zou et al. 2016). Closely linked SNP markers, or preferably markers based on target gene sequences, allow efficient incorporation of identified genes/QTL into cultivars by marker-assisted selection (MAS) and supplement conventional breeding with greater precision and hence reductions in time and costs (Xu et al. 2017).

The International Maize and Wheat Improvement Center (CIMMYT) stresses the importance of resistance diversity as a means of sustaining current yield levels as well as improving yield potential (Guzmán et al. 2017). During the last 30 years many wheat lines were imported from Mexico to China. In previous studies we have identified numerous lines with effective resistance to stripe rust in greenhouse and field environments from over 1000 common wheat accessions including CIMMYT germplasms (Han et al. 2012; Wu et al. 2018a; Zeng et al. 2014). Two CIMMYT-derived selection of advanced lines P10078 and Snb"S" have displayed high levels of APR to current Chinese *Pst* races since 2008. They may share a common ancestor (CIMMYT 1983; http://wgb.cimmyt.org/gringlobal/search.aspx). This investigation was planned to discover and map genomic regions containing APR QTL using SNP arrays following BSA, to identify specific SNPs or alleles in the target region of major QTL by haplotype analysis, and to develop KASP markers for marker-assisted selection in breeding programs.

Materials and methods

Plant materials

Two mapping populations were studied. The first population comprised of 124 F_6-derived F_7 recombinant inbred lines (RILs) from cross Mingxian 169 × P10078 (M/P); the other, 197 $F_{2:3}$ lines Zhengmai 9023 × Snb"S" (Z/S). P10078 (Moncho"S"/Imuris 79, CM61942-5Y-1M-1Y-1M-OY) and Snb"S" (Sunbird"S," CM 34630-D-3M-3Y-1M-1Y-OM) are two CIMMYT-derived selection of advanced lines and from the cross (We-Gto/Kal-Bb) × (Bucky/Maya74/4/Bluebird//HD832.5.5/Olesen/3/Ciano/Penjamo 62) and Gll-Cuc"S" × Kvz-Sx, respectively. Mingxian 169 (MX169) is a Chinese winter wheat landrace susceptible to all local *Pst* races. Zhengmai 9023 (ZM9023) is an elite wheat commercial cultivar, but it is moderate to highly susceptible to current prevalent *Pst* races (Xue et al. 2014). MX169, Avocet S (AvS) and Xiaoyan 22 (XY22) were used as additional susceptible controls. A diversity panel of 176 common wheat cultivars and landraces from around the world was screened in a SNP-based haplotype analysis using the Wheat660K array (Jia and Zhao 2016). The ultimate goal was to determinate the applicability of the specific SNP markers linked to identified QTL for marker-based selection. These materials

were obtained from the China Agriculture Research System (CARS).

Greenhouse trials

Seedling and adult plant tests were conducted under controlled greenhouse conditions to characterize the adult plant responses of P10078 and Snb"S". Seven *Pst* races (CYR29, CYR31, CYR32, CYR33, CYR34, Su11-7 and V26/CH42) were used. Their virulence/avirulence characteristics were reported by Wu et al. (2016). For seedling tests 10–15 plants of MX169, ZM9023, P10078 and Snb"S" were grown in 9 × 9 × 9 cm pots, and for adult plant tests three plants were grown in larger 20 × 20 × 15 cm pots. Seedlings at the two-leaf stage (14 days after planting) and adult plants at the booting stage were separately inoculated with urediniospores of each race mixed with talc (approximate ratio 1:20). Inoculated plants were incubated at 10 °C in a dew chamber in darkness for 24 h, and then transferred to a greenhouse at 17 ± 2 °C with 14 h of light (22,000 lx) daily. Infection types (IT) were recorded 18–21 days after inoculation using a 0–9 scale (Line and Qayoum 1992). Plants with ITs 0 to 6 were considered resistant, and plants with ITs 7 to 9 were considered susceptible. In order to confirm ITs, the tests were repeated three times.

Field test and phenotyping

All field plots were sown between October and early November during growing seasons (2015–2016 and 2016–2017). The mapping populations were planted in plots located near Yangling (YL: 34°17′N, 108°04′E, altitude 519 m) and Jiangyou (JY: 31°53′N, 104°47′E, altitude 571 m) in randomized complete blocks with two replications. Thirty seeds of each line were planted in a 1-m row with 25 cm between rows. The parents and susceptible check XY22 were planted after every 20 rows. The diversity panel was also grown in field nurseries near Yangling (YL) with two replications between 2008 and 2017 (Han et al. 2010, 2012, 2015; Zeng et al. 2014, 2015). Spreader rows containing mixtures of *Pst*-susceptible genotypes MX169 and AvS were planted around the plot area to assist the uniform increase and spread of inoculum throughout the field. Jiangyou is a part of an over-wintering region for natural stripe rust development, and nurseries grown there do not need to be artificially inoculated. The trials planted at Yangling were inoculated with a mixture of prevalent *Pst* races (CYR32 + CYR34) suspended in liquid paraffin (1:300) sprayed onto MX169 and AvS at flag leaf emergence. The parents along with progeny lines were visually rated for infection type and severity 18–20 days post-flowering when disease severity levels on susceptible checks had reached maximum levels of 90–100% (around 15–20 May at Yangling and 10–15 April at Jiangyou). IT data recorded for each line were based on a 0–9 scale (Line and Qayoum 1992). Disease severity was scored based on the modified Cobb scale (Peterson et al. 1948). IT and DS of homozygous lines were recorded as single values; and for segregating lines IT and DS were recorded as two or more values, but later averaged for each line.

DNA isolation, pool genotyping and molecular marker analysis

Fresh leaves of F_2 plants, F_6-derived progeny and their corresponding parental lines were collected at the jointing stage in the field. Genomic DNA samples were extracted using the method described in Song et al. (1994). Pooling of extreme phenotypes of $F_{2:3}$ lines and F_7 RILs in all environments was undertaken to generate DNA R-pools (IT 1–2, DS ≤ 10) and S-pools (IT 8–9, DS ≥ 90). Two pairs of R-pools versus S-pools were constructed, and each DNA pool contained equal amounts of DNA from five $F_{2:3}$ lines or RILs. DNA of the $F_{2:3}$ and F_7 pools, along with parental DNA, was sent to CapitalBio Corporation (Beijing; http://www.capitalbio.com) for analysis by Affymetrix Wheat660K SNP assay. SNP genotype calling and allele clustering were processed with the Affymetrix Genotyping Console™ (GTC) software. Three distinct clusters representing the AA, AB and BB genotypes expected for bi-allelic SNP segregation were identified using the default clustering algorithm implemented in GTC. Most of data were automatically clustered, while manual clustering was applied in cases of less clear separation. Monomorphic and inferior quality SNP loci with more than 10% missing values, ambiguous SNP calling, or minor allele frequencies below 5%, were excluded from further analysis. Polymorphic SNPs associated with resistance in BSA contained homozygous and heterozygous genotypes. Only homozygous genotype differences were localized to chromosomes when using the high-density 660K map (Cui et al. 2017; Wu et al. 2018d).

For a subset of SNPs polymorphic between two extreme pools and parents in each population, those SNPs in the target region were selected for conversion to KASP markers based on chromosome location. Wide-scale development of cost-efficient KASP assays was utilized to genotype the corresponding $F_{2:3}$ lines and F_7 RILs (LGC Genomics, Middlesex, UK). The procedures of SNP conversion to KASP markers and selective KASP assay were described previously (Ramirez-Gonzalez et al. 2015; Wu et al. 2017).

Statistical analysis of phenotypic data

Mean IT and DS of $F_{2:3}$ lines and F_7 RILs were used to examine the variance within individual environments. Analyses of variance (ANOVA) and Pearson's correlation

coefficients were performed using the "AOV" tool in the QTL IciMapping V 4.1 software package (Meng et al. 2015; Wang 2009; http://www.isbreeding.net/). Broad-sense heritability (h_b^2) of stripe rust resistance was estimated based on the equation $h_b^2 = \sigma_g^2/(\sigma_g^2 + \sigma_{ge}^2/e + \sigma_\varepsilon^2/re)$, where $\sigma_g^2 = (MS_f - MS_{fe})/re$, $\sigma_{ge}^2 = (MS_{fe} - MS_e)/r$ and $\sigma_\varepsilon^2 = MS_e$; σ_g^2 = genetic variance, σ_{ge}^2 = genotype × environment interaction variance, σ_ε^2 = error variance, MS_f = mean square of genotypes, MS_{fe} = mean square of genotype × environment interaction, MS_e = mean square of error, r = number of replications, and e = number of environments. For each trait, best linear unbiased estimation (BLUE) values were calculated across environments using the ANOVA function in IciMapping V4.0 software assuming fixed effects for the genotype.

Linkage and QTL analysis

Chi-squared (χ^2) tests for goodness of fit were performed to determine agreement of observed and expected segregation ratios. Linkage analysis and genetic map construction were established using the "MAP" tool with default parameters (Meng et al. 2015). Recombination frequencies between markers estimated by the Newton–Raphson method were converted to centimorgans (cM) using the Kosambi function (Kosambi 1943), and a LOD score of 3.0 was set as threshold (Wang 2009). The genetic linkage map was drawn with the software Mapchart V2.3 (Voorrips 2002). Chromosome bin assignment of a resistance locus in a linkage group was based on the physical positions of previously published expressed sequence tags (ESTs) in deletion maps (Qi et al. 2004; https://wheat.pw.usda.gov/cgi-bin/westsql/map_locus.cgi).

Inclusive composite interval mapping of the additive tool (ICIM-ADD) in IciMapping V 4.1 was carried out to detect QTL for IT and DS for both populations. A QTL analysis was conducted for either population per location, with the mean data across environments to determine balanced values for each line. Likelihood-of-odds (LOD) thresholds for declaring statistical significance were calculated by 1000 permutations at a p value ≤ 0.01. LOD significance thresholds estimated for each trait ranged from 3.5 to 5.2. The phenotypic variances explained (PVE) by individual QTL and additive effects at the LOD peaks were also obtained. Inclusive composite interval mapping of digenic epistatic QTL (ICIM-EPI) functionality was also used to detect epistatic interactions between QTL on chromosomes 6B and 2B for the Z/S population.

In silico mapping of 660K probe sequences to reference maps

In order to determine the physical position of polymorphic SNP markers on chromosome 6B, 660K SNP probes were aligned with respect to the newly released Chinese Spring sequence through a BLAST search (RefSeq v.1.0, IWGSC 2018). Filtering criteria were applied such that significant hits were required to obtain an expectation value (E) of $1e{-}10$. Probes from the Wheat660K SNP array that mapped to QTL intervals on chromosome 6B for the RIL and $F_{2:3}$ populations were compared to integrated maps provided by Dr. Fa Cui (Fa Cui, pers. comm.). The physical positions of the 660K probes within these intervals on IWGSC RefSeq chromosome 6BL were used to compare genetic and physical distances.

Haplotype analysis and specific KASP markers development

According to the deduced region of QTL on the integrated maps, the 660K SNP genotype data of 176 diverse wheat accessions were used to track haplotypes with specific genomic segments linked to the target QTL. Phylogenetic analysis was performed using software of MEGA v7.0.14. to cluster groups of markers, and lines based on genotypic similarity corresponding to phenotypes. All data were visualized using the visualize model online operation provided by the ITOL website (http://itol.embl.de/). Specific SNPs linked to the target QTL were then developed to KASP markers for using in marker-assisted selection.

Results

Progeny response at adult plant stage

Adequate disease levels were obtained in all experiments. Infection type and disease severity data for each line in both populations in each environment suggested that the data were continuously distributed characteristic of a quantitative trait (Fig. 1; Table S1). P values from ANOVA for both populations showed significant phenotypic variation in both IT and DS among lines, environments and line by environment interactions; no significant variation was detected among replications within experiments; line differences had the greatest effect on phenotypic variation; consequently, heritabilities and correlation coefficients between sites were high (Tables 1, 2). Thus, the expression of APR was consistent across environments, and QTL controlling APR had a very large effect on reducing stripe rust severity.

Pool analysis by Wheat660K SNP array

After genotyping the DNA pools by the Wheat660K SNP array, SNP variations were filtered and clustered. For the M/P RIL population there were 1451 common SNP variations between the two pairs DNA pools (Fig. 2a); 1109 of them were placed on chromosome (chr) 6B, and the others

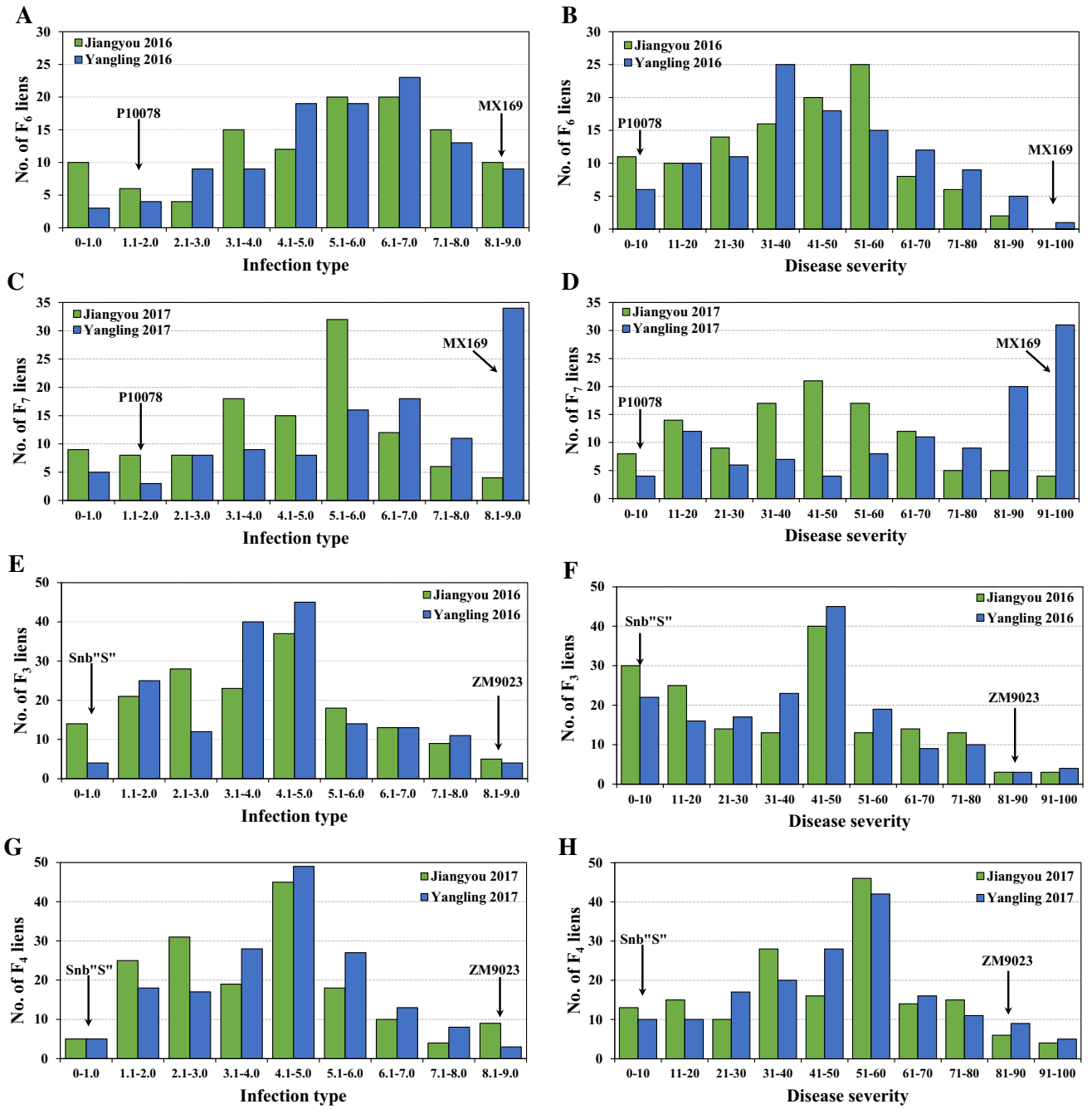

Fig. 1 Frequency distributions of mean infection types and disease severities for the 124 RILs from MX169×P10103 and the 197 $F_{2:3}$ lines from ZM9023×Snb"S" evaluated in Yangling and Jiangyou in 2015–2016 (**a**–**d**) and 2016–2017 (**e**–**h**). The values for the parents ZM9023, MX169 and P10103 are indicated by arrows

were distributed across other chromosomes (Fig. 2b). The proportion of SNPs overlapping between pools and parents showed the highest value (20.2%) for chr 6B (Fig. 2b). In the Z/S $F_{2:3}$ population, the two pairs DNA pools shared 3190 common SNP variations (Fig. 2c); 1374 and 1063 of these SNPs were located on chromosomes 6B and 2B, respectively; the proportion of SNPs overlapping between pools and parents also showed that the values for 6B (30.5%) and 2B (11.6%) were the highest (Fig. 2d). These results indicated that SNP variations on chr 6B for both populations were extremely likely to involve a major resistance locus and that there was another QTL on 2B in the Z/S $F_{2:3}$ population. When calculating the position distributions of these targeted SNPs, most of the linked SNPs on chr 6B

Table 1 Variance components of infection type (IT) and disease severity (DS) scores for RIL population derived from MX169 × P10078 (M/P) and $F_{2:3}$ population derived from ZM9023 × Snb"S" (Z/S) across four environments

Source of variation	IT			DS		
	Df	Mean square	*F* value	*Df*	Mean square	*F* value
RILs	123	44.23	132.50*	123	4375.14	73.17*
Replicates/environment	4	1.63	1.31	4	95.49	1.59
Environments	3	145.29	435.22*	3	31,689.99	530.00*
Line × environment	369	1.92	5.77*	369	307.36	5.14*
Error	492	0.34		492	59.79	
h_b^2	0.94			0.90		
$F_{2:3}$ lines	195	18.60	57.41*	195	2642.89	65.66*
Replicates/environment	4	4.87	15.03*	4	669.88	16.64*
Environments	3	14.99	46.25*	3	1750.77	43.50*
Line × environment	585	1.09	3.35*	585	129.10	3.21*
Error	780	0.32		780	40.25	
h_b^2	0.93			0.91		

*Significant at $P = 0.01$

Table 2 Correlation analysis (*r*) of mean disease severity (DS) and infection type (IT) of the MX169 × P10078 (M/P) RIL population and ZM9023 × Snb"S" (Z/S) $F_{2:3}$ population across four environments

Environment (location, year)	*r* values based on MDS (IT)[a]							
	YL2016 M/P	JY2016 M/P	YL2017 M/P	JY2017 M/P	YL2016 Z/S	JY2016 Z/S	YL2017 Z/S	JY2017 Z/S
YL2016 M/P	1							
JY2016 M/P	0.86 (0.92)	1						
YL2017 M/P	0.83 (0.86)	0.68 (0.71)	1					
JY2017 M/P	0.86 (0.90)	0.94 (0.95)	0.69 (0.71)	1				
YL2016 Z/S	–	–	–	–	1			
JY2016 Z/S	–	–	–	–	0.82 (0.80)	1		
YL2017 Z/S	–	–	–	–	0.82 (0.81)	0.81 (0.78)	1	
JY2017 Z/S	–	–	–	–	0.82 (0.79)	0.91 (0.89)	0.81 (0.77)	1

YL Yangling, *JY* Jiangyou

[a]*r* values calculated with IT are showed in parentheses. All *r* values were significant at $P = 0.001$

from the RIL population were within the physical interval of 519–632 Mb and two genetic intervals of 46–52 cM and 144–168 cM, respectively (Fig. 2e, f; Table S2A). Linked SNPs on chr 6B in the Z/S $F_{2:3}$ population were enriched in physical intervals 75–151 Mb and 480–686 Mb, respectively, corresponding to genetic intervals of 46–52 cM and 144–168 cM, respectively (Fig. 2g, h; Table S2B). In addition, linked SNPs on chr 2B were also clustered in physical intervals 53–117 Mb and 595–747 Mb, but corresponding to one genetic interval 50–94 cM (Fig. 2i, j; Table S2B). These combined results indicated that the overlapping interval on chr 6B in Z/S population likely harbored a major QTL and chr 2B a less effective QTL.

Linkage map and QTL detection

Fifty-two chromosome-specific SNPs in the overlapping region on chr 6B and 2B were selected for conversion to KASP markers and then screened on the parents and pools to confirm polymorphisms before being genotyped on the entire population; 23 failed to distinguish the contrasting pools along with the parents in the Z/S $F_{2:3}$ population. Sequences of the KASP markers are listed in Table S3. The first genetic map was constructed using the 14 KASP markers genotyped on the 197 F_2 plants, resulting in a linkage group on 2B spanning 20.8 cM (Fig. 3a). Using ICIM with the mean IT and DS data, the QTL *QYrsnb.nwafu-2BL* was identified and located in a 2.2-cM interval spanned by SNP markers *AX-109898885* and *AX-95658192*. (Figure 3a) It conferred moderate effect and explained 11.5–23.1% of the phenotypic variation across environments (Table 3). The second genetic map for chr 6B was constructed using 15 KASP markers. QTL *QYr.nwafu-6BL.2* flanked by markers *AX-109585549* and *AX-110989911* had the average peak LOD values of 34.6–44.3 (Fig. 3b; Table 3) and explained 42.7–52.5% of the phenotypic variation (Table 3).

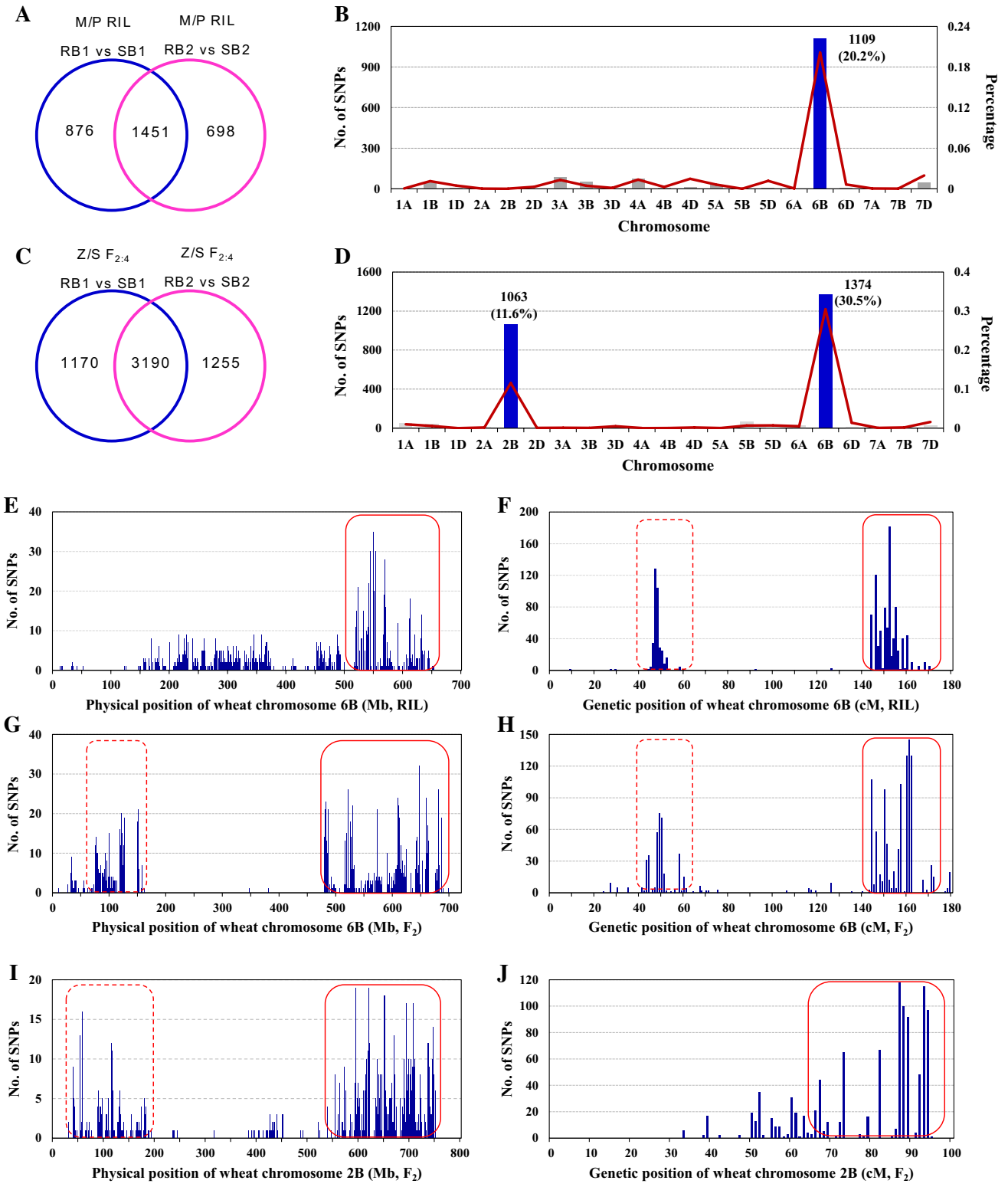

Fig. 2 Overview of analyses of 660K SNP arrays. **a**, **c** Venn diagrams of polymorphic SNPs; **b**, **d** distribution of polymorphic SNPs in each chromosome based on 660K genetic maps; **e**, **g**, **i** physical positions of polymorphic SNPs in the chr 6B and 2B reference genomes were determined by best alignment to IWGSC RefSeq v1.0; **f**, **h**, **j** genetical positions of polymorphic SNPs in the chr 6B and 2B reference genetic maps were provided by Prof. Jizeng Jia. SNPs were clustered by location (windows size: 1 Mb and 1 cM, respectively), and selected SNPs (in red boxes) were analyzed in KASP assays (color figure online)

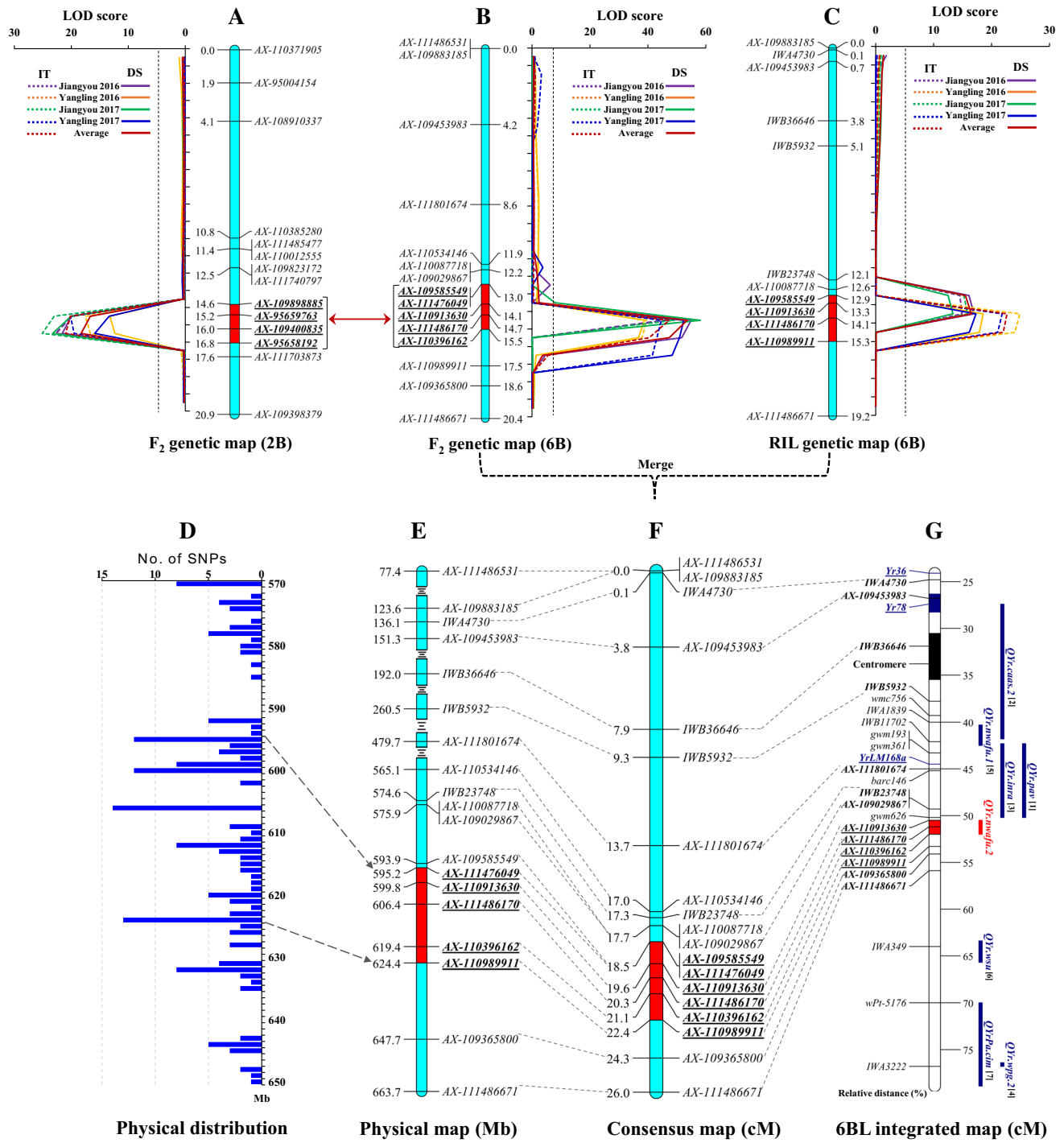

Fig. 3 Graphical displays of locations of QTL for stripe rust resistance across all environments for the ZM9023 × Snb"S" (Z/S) and MX169 × P10078 (M/P) populations. Genetic linkage maps of QYrsnb.nwafu-2BL and QYr.n*wafu-6BL.2* produced from results of by using Z/S $F_{2:3}$ lines (**a**, **b**) and M/P RILs (**c**). Markers surrounding the QTL are in underlined, bold font. Connecting lines with double-ended arrows denoted epistatic interaction between markers/QTL. **d** Physical positions of polymorphic SNPs in the target region of chromosome 6B were clustered by slide window (size: 1 Mb). **e** Physical map of wheat chromosome 6B constructed using polymorphic markers from selected SNPs analyzed in KASP assays. **f** Consensus map of chromosome 6B constructed by linkage maps from Z/S and M/P. **g** Identified QTL (red bar and underlined font and red region on chromosome 6B) in this study and previously mapped *Pst* resistance genes and QTLs (blue bars) were positioned based on integrated genetic maps. Centromere region is colored black. Confidence intervals of QTLs are indicated with blue lines. References [1] William et al. (2006), [2] Lan et al. (2010), [3] Dedryver et al. (2009), [4] Hou et al. (2015), [5] Wu et al. (2018b), [6] Bulli et al. (2016) and [7] Rosewarne et al. (2013) (color figure online)

The third genetic map was constructed for the M/P RIL population using 12 markers on chr 6B (Fig. 3c). Of these markers some were from the wheat 90K SNP array in a previous study (Wu et al. 2018b). The marker order for the RIL genetic map was similar to that for the $F_{2:3}$ population (Fig. 3b, c). The QTL on 6B was also detected by ICIM, and the corresponding variances explained ranged from 30.0 to 59.7% across environments (Table 3). *QYr.nwafu-6BL.2* was also in the marker interval between *AX-109585549* and *AX-110989911* spanning 2.4 cM. According to the position of the ESTs in the 2B and 6B deletion bin map, *QYrsnb.nwafu-2BL* and *QYr.nwafu-6BL.2* were likely located in bins 2BL4-0.50-0.89 and 6BL5-0.40-1.00, respectively (Table S4).

QTL analysis

To assess resistance effects conferred by each QTL alone or in combination, the lines were divided into genotypic groups based on the presence/absence of the most closely linked flanking markers. M/P RILs were divided into two groups: those carrying *QYr.nwafu-6BL.2* and those without. The mean infection types and disease severities for lines carrying this locus (+*QYr.nwafu-6BL.2*) ranged from 0.8 to 6.9 and 2 to 69.4%, respectively, whereas for those without this QTL (−*QYr.nwafu-6BL.2*) ranged from 2.5 to 9.0 and 23.8 to 91.9%, respectively (Fig. 4a–d; Table S1A). QTL *QYr.nwafu-6BL.2* reduced stripe rust severity by 27.2 to 40.1% (Table S5A). On the other hand, there was a significant epistatic effect for stripe rust resistance in $F_{2:3}$ lines. The *QYr.nwafu-6BL.2* + *QYrsnb.nwafu-2BL* combination produced a positive epistatic effect with PVE 71.2–79.9% (Table 4); the corresponding stripe rust infection types and severities ranged from 0.5 to 2.5, and 1.0 to 21.3%, respectively, across the environments, lower than those with only one QTL, but visually identical to the resistant parent (Fig. 4e, f; Table S5B). All of the above results were obtained using the BIP functionality of the QTL IciMapping V 4.1 software for significant epistatic effects ($P < 0.01$).

Haplotype analysis and development diagnostic markers

The genomic segment of *QYr.nwafu-6BL.2* containing 46 SNPs was extracted from 176 wheat accessions with 660K SNP genotyping data to observe haplotype and phylogenetic clustering (Table S6). The diversity panel based on the *QYr.nwafu-6BL.2* interval using the SNP data revealed three distinct clusters. As shown in Fig. 5 and Table S6, the branch for the target region of line P10078 and Snb"S" is considerably differentiated from the other branches for the corresponding regions in lines without the target QTL. Accessions within this branch displayed adult plant resistance in the field tests suggesting that they possibly contained the same locus. Pedigree analysis demonstrated again that

Table 3 Summary of stripe rust resistance QTL detected by ICIM in the MX169 × P10078 (M/P) RIL population and ZM9023 × Snb"S" (Z/S) $F_{2:3}$ population across four environments

Environment	Position[a]	Marker interval	IT			DS		
			LOD	Add	PVE	LOD	Add	PVE
QYr.nwafu-6BL.2								
YL2016 M/P	15	*AX-111486170–AX-110989911*	24.7	−2.0	59.7	18.3	−17.2	50.2
JY2016 M/P	13	*AX-109585549–AX-110913630*	14.9	−1.7	43.4	16.9	−18.8	46.8
YL2017 M/P	14	*AX-110913630–AX-111486170*	21.8	−1.8	55.6	17.3	−19.0	48.0
JY2017 M/P	13	*AX-109585549–AX-110913630*	15.6	−1.7	44.7	9.1	−14.1	30.0
Mean	14	*AX-110913630–AX-111486170*	22.1	−1.8	56.8	16.1	−15.8	45.8
QYr.nwafu-6BL.2								
YL2016 Z/S	15	*AX-111486170–AX-110396162*	39.5	−1.5	50.3	38.8	−18.8	51.9
JY2016 Z/S	15	*AX-111486170–AX-110396162*	44.3	−1.9	52.5	37.8	−24.0	48.4
YL2017 Z/S	15	*AX-111486170–AX-110396162*	34.6	−1.6	42.7	42.4	−19.4	51.6
JY2017 Z/S	14	*AX-111476049–AX-110913630*	39.0	−1.8	45.5	47.0	−22.2	48.0
Mean	15	*AX-111486170–AX-110396162*	36.8	−1.7	45.3	42.8	−21.1	50.0
QYrsnb.nwafu-2BL								
YL2016 Z/S	15	*AX-109898885–AX-95659763*	17.5	−0.9	17.2	13.2	−9.9	13.4
JY2016 Z/S	16	*AX-109400835–AX-95658192*	20.1	−1.0	14.6	18.7	−10.5	11.8
YL2017 Z/S	16	*AX-109400835–AX-95658192*	19.5	−0.9	16.8	15.9	−8.6	11.5
JY2017 Z/S	16	*AX-109400835–AX-95658192*	23.1	−1.2	18.6	22.9	−14.3	18.1
Mean	16	*AX-109400835–AX-95658192*	20.5	−1.0	17.3	20.1	−10.8	15.0

[a]Peak position in centimorgans from the first linked marker of the relevant linkage group

LOD logarithm of odds score, *Add* additive effect of the resistance allele and *PVE* percentage of phenotypic variance explained by individual QTL

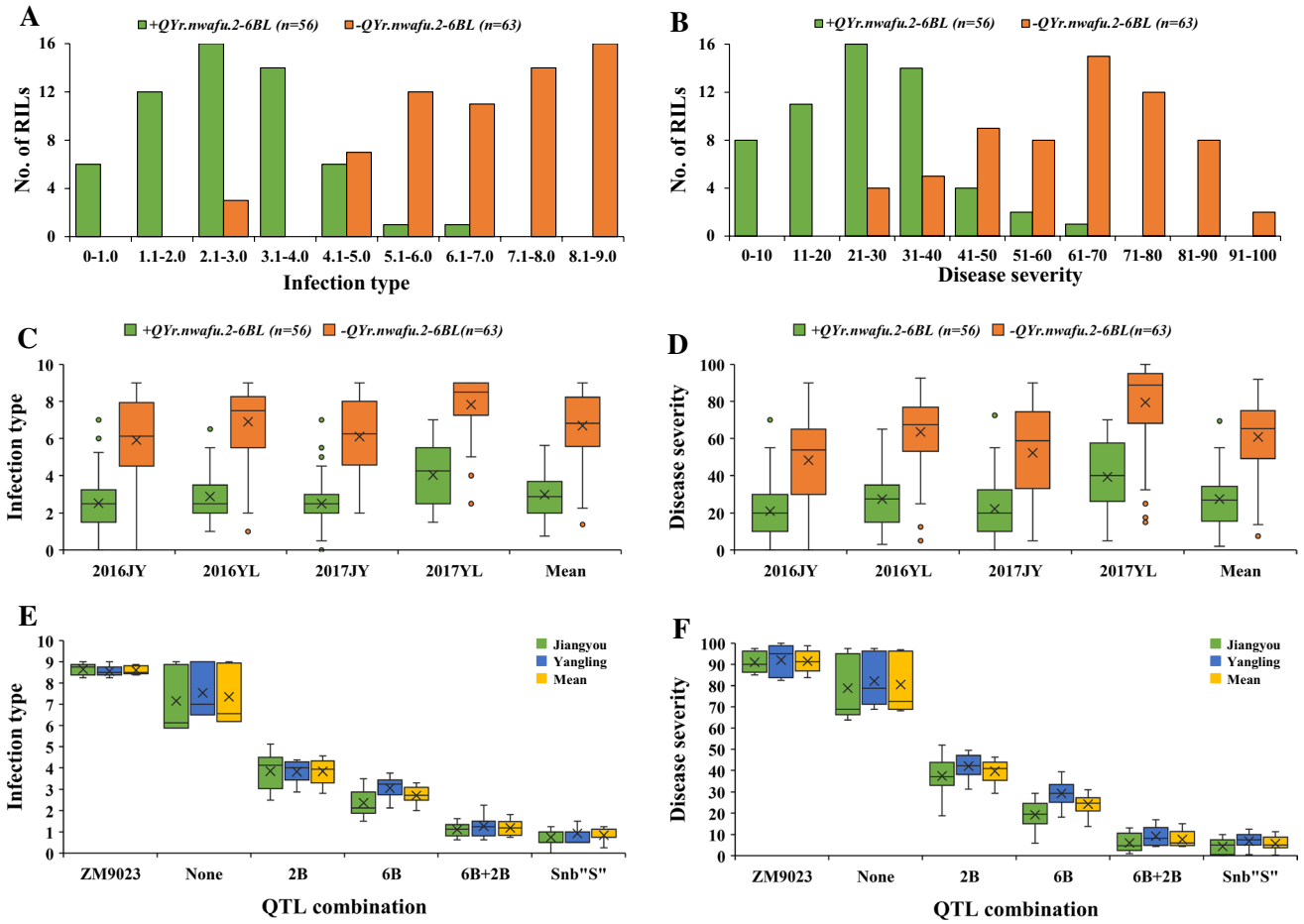

Fig. 4 Effects of single QTL and their combination on stripe rust scores illustrated by the average infection type and disease severity of RILs from MX169×P10078 (**a**, **b**) in Yangling, Jiangyou and combined environments (**c**, **d**); and from ZM9023×Snb"S" (**e**, **f**). The box plots (quartiles are boxes, medians are continuous lines, means are crosses, whiskers extend to the farthest points; outliers are represented by black dots) for infection type and disease severity associated with the two QTL (2B and 6B) and their combination

Table 4 Summary of the epistatic interactions detected using inclusive composite interval mapping of digenic epistatic QTL (ICIM-EPI) functionality in the Z/S population among identified QTLs, phenotypic variance by locations and arithmetic means across environments

Environment	Epistatic interaction	Epistatic LOD	Epistatic PVE	Add1	Add2	Add1 by Add2
Infection type						
YL2016 Z/S	*2BL×6BL*	8.2	78.8	−1.63	−1.41	0.63
JY2016 Z/S	*2BL×6BL*	8.6	79.9	−1.20	−1.20	0.56
YL2017 Z/S	*2BL×6BL*	7.7	71.2	−1.95	−0.47	0.39
JY2017 Z/S	*2BL×6BL*	8.1	75.4	−1.10	−0.82	0.45
Mean	*2BL×6BL*	7.9	73.6	−1.05	−1.23	0.42
Disease severity						
YL2016 Z/S	*2BL×6BL*	6.9	79.4	−10.51	−15.4	6.53
JY2016 Z/S	*2BL×6BL*	6.8	78.4	−10.13	−12.16	5.67
YL2017 Z/S	*2BL×6BL*	6.6	74.3	−22.12	−5.16	4.80
JY2017 Z/S	*2BL×6BL*	6.9	79.2	−13.43	−10.12	6.51
Mean	*2BL×6BL*	6.7	75.7	−12.52	−9.36	5.12

LOD logarithm of odds score, *PVE* percentage of phenotypic variance explained by individual QTL and *Add* additive effect of the resistance allele

almost all accessions identical to P10078 and Snb"S" were CIMMYT derivatives (CIMMYT 1983). The haplotypes were not associated with phenotypic values in other branches indicating that these accessions may not carry the *QYr. nwafu-6BL.2* allele (Fig. 5). All SNP alleles were located in the 595.2–624.4-Mb interval of the IWGSC chromosome 6B (Fig. 3d); their combinations could properly differentiate the target group from other groups in the panel such as *AX-111634916* (G/C) and *AX-110564148* (G/A) or *AX-86165412* (T/G) and *AX-108971472* (T/C) (Fig. 5, Table S6).

In addition, these 176 wheat accessions were also used to assess the robustness of KASP markers linked to *QYrsnb. nwafu-2BL* for marker-assisted selection. Although markers *AX-109898885* (T/C), *AX-109400835* (T/C), *AX-95659763* (G/T) and *AX-95658192* (T/G) failed to distinguish resistant and susceptible lines separately (Table S6), the combination of the three closest markers (*AX-109898885*, *AX-95659763* and *AX-95658192*) should be available. Those lines carrying positive alleles associated with *QYrsnb.nwafu-2BL* were derived from CIMMYT germplasms (CIMMYT 1983).

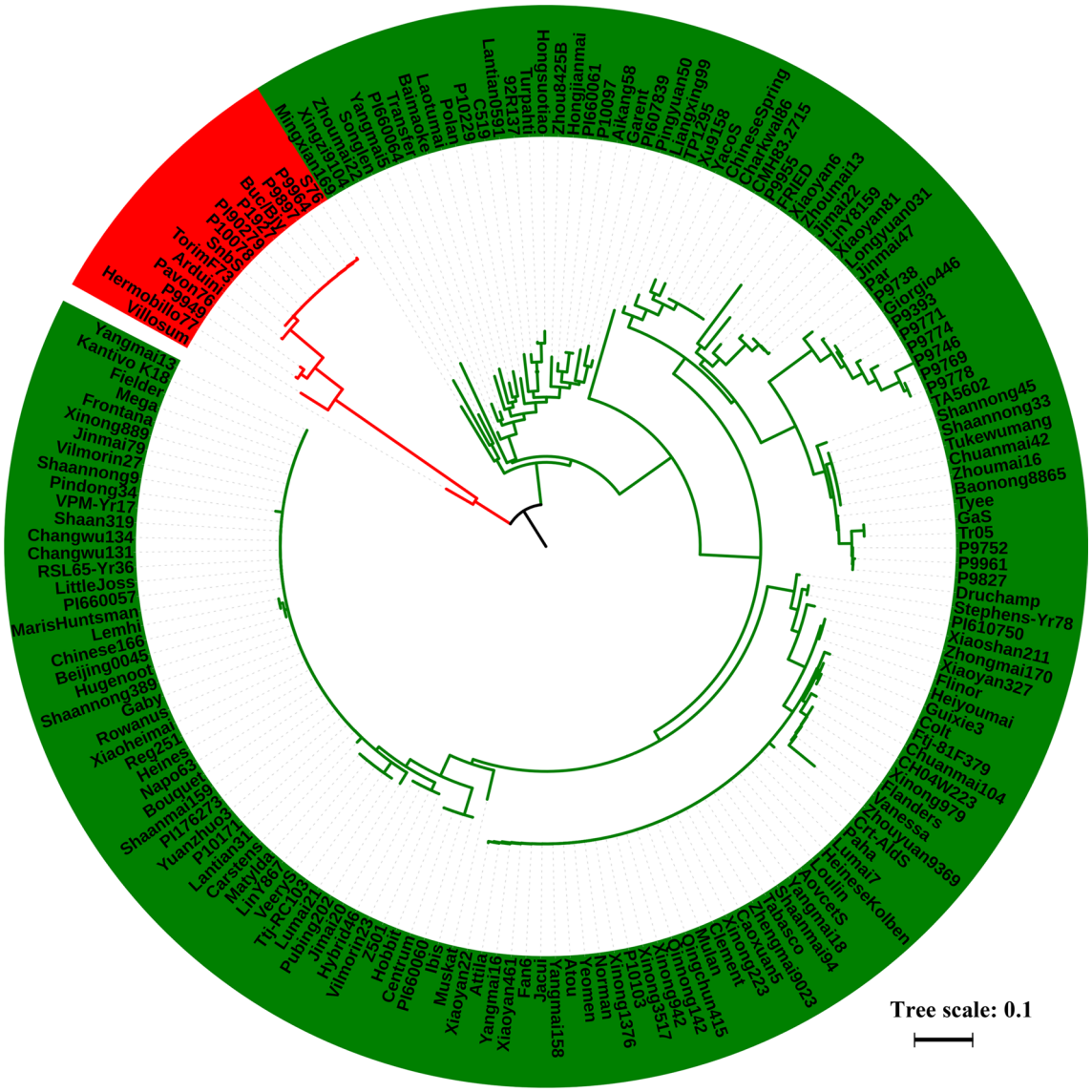

Fig. 5 Haplotype variation of the *QYr.nwafu-6BL.2* region among the set of wheat genotypes revealed by SNPs distributed in the target region (the red cluster). Phylogenetic tree constructed with SNPs embracing the *QYr.nwafu-6BL.2* region. Each accession in the tree was according to the topological structure groups. The details of results based on Wheat660K SNP markers are in supplementary Table S6 (color figure online)

Discussion

Recently identified Chinese *Pst* race groups, such as race CYR34 (*Yr26*-virulent group) with broader virulence profiles and increased aggressiveness, threaten cultivars with *Yr26* (Bai et al. 2017; Han et al. 2015; McIntosh et al. 2018). To expand and enrich the genetic resources for resistance to CYR34, more than 1000 common wheat accessions were screened and several potentially valuable resistance sources were identified (Han et al. 2012; Zeng et al. 2014). In the present study, we confirmed that two CIMMYT-derived wheat lines have adult plant resistance to stripe rust. We subsequently performed a genetic dissection and identified a common QTL in chromosome 6BL in accessions P10078 and Snb"S." A second QTL on was detected on 2BL in Snb"S."

Relationship between *QYr.nwafu-6BL.2* and other genes/QTL on 6BL

Five *Yr* genes are located on chromosome arm 6BS, namely *Yr35*, *Yr36*, *Yr78* and *YrLM168a*. Since all of these genes were on 6BS, they be different from *QYr.nwafu-6BL.2* on chromosome arm 6BL. However, several stripe rust APR QTLs on 6BL have been reported (Bulli et al. 2016; Rosewarne et al. 2013). To estimate the distance of *QYr.nwafu-6BL.2* from other resistance genes/QTLs on 6BL, comparisons were made based on two integrated genetic maps. The first consisted of SSR markers and the Wheat90K SNP array (Maccaferri et al. 2015), and the second contained known PCR markers (SSR, EST, STS, RAPD and RFLP), DArT, SNPs from Wheat90K, Wheat660K and Wheat820K SNP arrays (Fa Cui, pers. comm.). All genes/QTL were placed in an integrated genetic map based on the locations of flanking markers. Most of them were concentrated in the interval 40.1 to 50.1 relative distance (corresponding to an of interval 78.4–97.8 cM, total map length 195.2 cM), whereas *QYr. nwafu-6BL.2* spanned an interval from 89.5 to 90.6 cM, thus overlapping to some degree (Fig. 3g). In this interval, APR gene *YrLM168a* in CIMMYT cultivar Milan was flanked by SSR markers *Xwmc756* and *Xbarc146* (Feng et al. 2015). Milan, a derivative of French wheat VPM1 was selected from cross "*Aegilops ventricosa*/*T. persicum*//3 * T/*aestivum* cv. Marne" (Doussinault and Dosba 1981). Likewise, Dedryver et al. (2009) identified *QYr.inra-6B* in the same region in cultivar Renan, another VPM1 derivative, indicating that *QYr.inra-6B* and *YrLM168a* may be the same. *QYr.nwafu-6BL.1* with large effect was mapped in a German cultivar Friedrichswerther, which has APR to all Chinese races (Wu et al. 2018b). *QYrpav.cim-6BL* was identified in CIMMYT cultivar Pavon 76 closed to marker *XPstAGGMseCGA1* (William et al. 2006). *QYrpin.caas.2-6BS* was characterized in an old Chinese cultivar Pingyuan 50 linked to markers *Xgwm361* and *Xbarc136* (Lan et al. 2010). Based on integrated genetic map, *YrLM168a, QYr.nwafu-6BL.1* and *QYrpin.caas.2-6BS* were more than 10 cM from *QYr. nwafu-6BL.2*; *QYrpav.cim-6BL* shared an overlapping region; and other QTLs such as *QYr.wsu-6B*, *QYrpas.cim-6B* and *QYr.wpg-6B.2* were more than 20 cM from *QYr. nwafu-6BL.2*. *QYr.nwafu-6BL.1* and *QYr.nwafu-6BL.2* are located in bins 6BL3-0-0.36 and 6BL5-0.40-1.00, respectively, based on the physical positions of ESTs in 6BL chromosomal bins. In our study, when tested with *Pst* race CYR34 in the greenhouse P10078, and Snb"S," their progenies, Druchamp and Friedrichswerther, showed moderate or high resistance at the adult plant stage, whereas Pavon 76, VPM1, LM168a, Renan and Pingyuan 50 were slow rusting with disease severities of 40–80% (Wu et al. 2018b). In addition, SSR markers linked with previously reported genes/QTLs in chromosome 6B were evaluated on MX169, ZM9023, P10078, Snb"S" and wheat lines with the corresponding QTL in order to determine if *QYr. nwafu-6BL.2* was unique. None of the markers flanking these QTLs showed polymorphism in our population, and haplotype analysis using SNP alleles surrounding *QYr. nwafu-6BL.2* differentiated the target group from other wheat lines except Pavon 76 (Fig. 5, Table S6). Thus, *QYr. nwafu-6BL.2* appears to be new or similar to *QYrpav.cim-6BL* based on comparison of relative distance, stripe rust responses, pedigree analyses and molecular analysis, but allelism tests, cloning or precise phenotypic comparisons will be needed for confirmation.

QTL on chromosome 2BL and QTL interaction

QYrsnb.nwafu-2BL with flanking markers *AX-109898885* and *AX-95658192* was identified in Snb"S." Several genes (*Yr3*, *Yr5*, *Yr7, Yr43*, *Yr44* and *Yr53*) were reported previously in chromosome 2BL, and all confer all-stage resistance (Maccaferri et al. 2015). Most of these genes, except *Yr5* and *Yr53*, are ineffective to Chinese *Pst* races (Zeng et al. 2015). *Yr5* is derived from *Triticum aestivum* ssp. *spelta* var. *album* (Macer 1966) and was mapped in an interval between SNP markers *IWA6121* and *IWA4096* (Naruoka et al. 2016). *Yr53* originally from durum wheat PI 480148 was flanked by *Xwmc441* and *XLRRrev/NLRRrev350* (Xu et al. 2013). *QYrsnb.nwafu-2BL* from common wheat confers resistance in adult plants indicating that *QYrsnb.nwafu-2BL* is different from *Yr5* and *Yr53*. Several stripe rust QTLs on chromosome arm 2BL have been reported and located in a similar region (Rosewarne et al. 2013), i.e., *QYrdr.wgp-2BL* in Druchamp, *QYr.caas-2BL* in Naxos, *QYraq.cau-2BL* in Aquileja and

QYr.inra-2BL in Camp Remy and *QYrqin.nwafu-2BL* in Qinnong 142 (Guo et al. 2008; Hou et al. 2015; Mallard et al. 2005; Ren et al. 2012; Zeng et al. 2018). *QYrdr.wgp-2BL* was identified as a minor QTL explaining 4.0–10.8% of the phenotypic variance with its linked SNP marker *IWA7583* (Hou et al. 2015). *QYr.caas-2BL* also with minor effect was detected in a larger interval between SSR markers *Xwmc441* and *Xwmc361* (Ren et al. 2012). *QYraq.cau-2BL* accounting for 61.5% of the phenotypic variance was located in the marker interval *Xwmc175-Xwmc332* (Guo et al. 2008). *QYr.inra-2BL*, contributing up to 61% of the phenotypic variance, was flanked by *Xbarc101* and *Xgwm120* (Mallard et al. 2005). Based on the integrated genetic map all of these QTL are located in a close proximity to *QYrsnb.nwafu-2BL* indicating that there may be commonality of at least some of them, but only further comparative laboratory and field tests will provide more clarity. Moreover, we also observed synergistic interaction between *QYr.nwafu-6BL.2* and *QYrsnb.nwafu-2BL* such that the presence of both QTL conferred a higher level of resistance than either QTL alone. Such favorable combinations are likely to be common because breeders select for the highest levels of resistance in breeding populations.

Putative candidate genes contributing to APR

In the Z/S population *QYr.nwafu-6BL.2* was flanked by SNP markers *AX-109585549* and *AX-110396162*; in the M/P population, it was in the interval *AX-109585549–AX-110989911*. As both populations shared many common KASP markers and marker order, they were merged into a single consensus genetic map (Fig. 3f). *QYr.nwafu-6BL.2* was initially located in the interval *AX-109585549–AX-110989911*. According to the physical positions of SNPs (IWGSC RefSeq v1.0), this interval corresponds to 30.5 Mb (Table S7). Further analysis of the 8 environmental phenotypic values for both populations along with the genetic maps indicated that most of LOD peaks were located in the *AX-110913630–AX-111486170* overlapping confidence interval (Fig. 3b, c, e; Table 3 spanning about 6.6 Mb (6B: 599,879,663–6B: 606,426,279)). This interval harbors 35 high confidence gene models based on the current version of the IWGSC RefSeq v1.0 annotation. Of these functionally annotated genes, four candidate types for disease response were notable (Table S7). The gene *TraesCS6B01G340900.1* is predicted to confer a typical disease resistance protein with an NB-ARC motif and ADP-binding domain. The protein encoded by *TraesCS6B01G344000* is corresponding to universal stress protein which responses to stress. The genes *TraesCS6B01G341100*, *TraesCS6B01G341200*, *TraesCS6B01G341300* and *TraesCS6B01G341500* encode a GDSL esterase/lipase, which was reported to regulate systemic resistance associated with ethylene signaling in Arabidopsis (Kwon et al. 2009). *TraesCS6B01G342100.1* was annotated as hexosyltransferase. Sugars are involved in many metabolic and signaling pathways in plants. Sugar signaling may also contribute to immune responses against pathogens as changing concentrations or ratios of sugars in plant tissue induce plant defense genes, influence plant hormone pathways and induce resistance to diseases (Bolouri Moghaddam and Van den Ende 2012; Periyannan et al. 2017). Their function in energy metabolism and transport is exemplified by *Lr67/Yr46*, which confers APR to multiple fungal diseases. This gene encodes a hexose transporter that inhibits hexose uptake by host cells from the apoplast (Moore et al. 2015). Prediction of candidate genes sets a basis for the next step of map-based cloning of *QYr.nwafu-6BL.2*. Nevertheless, further genetic studies and more detailed analyses are needed to confirm the roles of this and other candidate genes in stripe rust response.

Haplotype analysis and its application for MAS in wheat breeding

Recent developments in genome sequencing enable generation of markers, such as SNP to provide high resolution of genetic diversity. The wheat 660K SNP array provides an extremely rich avenue of inquiry of natural variation in germplasm and permits identification of SNPs tightly linked to target genes/QTL. To identify haplotypes involved in stripe rust resistance and evaluate the robustness of markers linked to *QYr.nwafu-6BL.2,* 46 SNP markers surrounding the *QYr.nwafu-6BL.2* locus were extracted to generate SNP genotypic data from 176 diverse wheat genotypes. The target region in lines P10078 and Snb"S" was different from regions reported for QTL in other studies. The accessions from this group with P10078 and Snb "S" shared the same haplotype as P10078 and Snb"S," and they exhibited comparable adult plant resistance to stripe rust in the field tests indicating that they may contain *QYr.nwafu-6BL.2*. Pedigree analysis demonstrated that most of them were CIMMYT derivatives or associated with the CIMMYT breeding program (CIMMYT 1983). Most importantly, we have found the combinations of some SNP markers could differentiate the target group from other groups in the panel such as *AX-111634916* (G/C) and *AX-110564148* (G/A) or *AX-86165412* (T/G) and *AX-108971472* (T/C) (Table S6). Additionally, the QTL on 2BL with its flanking markers *AX-109898885*, *AX-95659763* and *AX-95658192* effectively distinguished the presence/absence of *QYrsnb.nwafu-2BL* when used in combination. This makes it possible to select the favorable haplotype associated with *QYr.nwafu-6BL.2* and *QYrsnb.nwafu-2BL* in wheat breeding by use of KASP markers.

Conclusions

This study identified a consistent and stable QTL for stripe rust resistance co-localized in a 3.9-cM interval on chromosome arm 6BL in two crosses and another QTL on chromosome 2B in one of them. The two QTL conferred higher resistance when combined. To elucidate the relationship between the genetic and physical maps of *QYr. nwafu-6BL.2*, 660K probes within the target region were anchored to the IWGSC RefSeq v.1.0. In further analysis of the locations of LOD peaks, the overlapping confidence interval was narrowed positions 599.9–606.4 Mb. This QTL region provides an opportunity for further map-based cloning, and the unique haplotypes identified will enable marker-assisted selection.

Author contribution statement QZ and JW conducted the experiments, analyzed the data and wrote the manuscript. SL and SY assisted in analyzing the data and preparing figures for the manuscript. QW and DH identified the resistant parental line, made the cross and participated in field experiments. SL, SH and JM participated in field experiments and contributed to genotyping. QZ, DH and ZK conceived and directed the project and revised the manuscript. All authors read and approved the final manuscript.

Acknowledgements The authors are grateful to Prof. R. A. McIntosh, Plant Breeding Institute, University of Sydney, for review of this manuscript. Dr. Jianhui Wu thanks Mr Yue Liu for participating in making the figures. This study was financially supported by the National Science Foundation for Young Scientists in China (Grant 31701421), the Genetically Modified Organisms Breeding Major Project (2016ZX08002001), and the earmarked fund for Modern Agro-industry Technology Research System (No. CARS-3-1-11).

Compliance with ethical standards

Conflict of interest The authors declare no competing interests.

Ethical standard I declare on behalf of my co-authors that the work described is original, previously unpublished research, and not under consideration for publication elsewhere. The experiments in this study comply with the current laws of China.

References

Abberton M, Batley J, Bentley A, Bryant J, Cai H, Cockram J, Costa De Oliveira A, Cseke LJ, Dempewolf H, De Pace C, Edwards D, Gepts P, Greenland A, Hall AE, Henry R, Hori K, Howe GT, Hughes S, Humphreys M, Lightfoot D, Marshall A, Mayes S, Nguyen HT, Ogbonnaya FC, Ortiz R, Paterson AH, Tuberosa R, Valliyodan B, Varshney RK, Yano M (2016) Global agricultural intensification during climate change: a role for genomics. Plant Biotechnol J 14:1095–1098

Bai BB, Liu TG, Liu B, Gao L, Chen WQ (2017) High relative parasitic fitness of G22 derivatives is associated with the epidemic potential of wheat stripe rust in China. Plant Dis 102:483–487

Bolouri Moghaddam MR, Van den Ende W (2012) Sugars and plant innate immunity. J Exp Bot 63:3989–3998

Brummer EC, Barber WT, Collier SM, Cox TS, Johnson R, Murray SC, Olsen RT, Pratt RC, Thro AM (2011) Plant breeding for harmony between agriculture and the environment. Front Ecol Environ 9:561–568

Bulli P, Zhang J, Chao S, Chen X, Pumphrey M (2016) Genetic architecture of resistance to stripe rust in a global winter wheat germplasm collection. G3 6:2237–2253

Chen XM (2013) High-temperature adult-plant resistance, key for sustainable control of stripe rust. Am J Plant Sci 04:608–627

Chen XM (2014) Integration of cultivar resistance and fungicide application for control of wheat stripe rust. Can J Plant Pathol 36:311–326

Chen XM, Kang ZS (2017) Stripe rust. Springer, Dordrecht, p 723

Chen WQ, Wu LR, Liu TG, Xu SC, Jin SL, Peng YL, Wang BT (2009) Race dynamics, diversity, and virulence evolution in *Puccinia striiformis* f. sp. *tritici*, the causal agent of wheat stripe rust in China from 2003 to 2007. Plant Dis 93:1093–1101

CIMMYT (1983) Report on Wheat Improvement. International Maize and Wheat Improvement Center, Mexico, p 20

Cui F, Zhang N, Fan X, Zhang W, Zhao C, Yang L, Pan R, Chen M, Han J, Zhao X, Ji J, Tong Y, Zhang H, Jia J, Zhao G, Li J (2017) Utilization of a Wheat660K SNP array-derived high-density genetic map for high-resolution mapping of a major QTL for kernel number. Sci Rep 7:3788

Dedryver F, Paillard S, Mallard S, Robert O, Trottet M, Negre S, Verplancke G, Jahier J (2009) Characterization of genetic components involved in durable resistance to stripe rust in the bread wheat 'Renan'. Phytopathology 99:968–973

Doussinault G, Dosba F (1981) Analyse monosomique de la résistance a la rouille jaune du géniteur blé tendre VPM 1. Comptes rendus des seances de l'Academie d'agriculture de France, pp 133–138

Ellis JG, Lagudah ES, Spielmeyer W, Dodds PN (2014) The past, present and future of breeding rust resistant wheat. Front Plant Sci 5:1–13

Feng J, Chen G, Wei Y, Liu Y, Jiang Q, Li W, Pu Z, Lan X, Dai S, Zhang M, Zheng Y (2015) Identification and mapping stripe rust resistance gene *YrLM168a* using extreme individuals and recessive phenotype class in a complicate genetic background. Mol Genet Genom 290:2271–2278

Giovannoni JJ, Wing RA, Ganal MW, Tanksley SD (1991) Isolation of molecular markers from specific chromosomal intervals using DNA pools from existing mapping populations. Nucleic Acids Res 19:6553–6568

Guo Q, Zhang ZJ, Xu YB, Li GH, Feng J, Zhou Y (2008) Quantitative trait loci for high-temperature adult-plant and slow-rusting resistance to *Puccinia striiformis* f. sp. *tritici* in wheat cultivars. Phytopathology 98:803–809

Guzmán C, Autrique E, Mondal S, Huerta-Espino J, Singh RP, Vargas M, Crossa J, Amaya A, Peña RJ (2017) Genetic improvement of grain quality traits for CIMMYT semi-dwarf spring bread wheat varieties developed during 1965–2015: 50 years of breeding. Field Crop Res 210:192–196

Han D, Wang Q, Zhang L, Wei G, Zeng Q, Zhao J, Wang X, Huang L, Kang Z (2010) Evaluation of resistance of current wheat cultivars to stripe rust in Northwest China, North China and the Middle and Lower Reaches of Changjiang River epidemic area. Sci Agric Sin 43:2889–2896 **(in Chinese with English summary)**

Han D, Zhang P, Wang Q, Zeng Q, Wu J, Zhou X, Wang X, Huang L, Kang Z (2012) Identification and evaluation of resistance to

stripe rust in 1980 wheat landraces and abroad germplasm. Sci Agric Sin 45:5013–5023 **(in Chinese with English summary)**

Han DJ, Wang QL, Chen XM, Zeng QD, Wu JH, Xue WB, Zhan GM, Huang LL, Kang ZS (2015) Emerging *Yr26*-virulent races of *Puccinia striiformis* f. sp. *tritici* are threatening wheat production in the Sichuan Basin, China. Plant Dis 99:754–760

Hou L, Chen X, Wang M, See DR, Chao S, Bulli P, Jing J (2015) Mapping a large number of QTL for durable resistance to stripe rust in winter wheat Druchamp using SSR and SNP markers. PLoS ONE 10:e01267945

Hovmøller MS (2007) Sources of seedling and adult plant resistance to *Puccinia striiformis* f. sp. *tritici* in European wheats. Plant Breed 126:225–233

Hovmøller MS, Walter S, Justesen AF (2010) Escalating threat of wheat rusts. Science 329:369

IWGSC (2018) Shifting the limits in wheat research and breeding using a fully annotated reference genome. Science 361:eaar7191

Jia J, Zhao G (2016) Wheat660 SNP array developed by CAAS. http://wheat.pw.usda.gov/ggpages/topics/Wheat660_SNP_array_developed_by_CAAS.pdf. Accessed 19 Feb 2018

Kosambi DD (1943) The estimation of map distances from recombination values. Ann Eugen 12:172–175

Kwon SJ, Jin HC, Lee S, Nam MH, Chung JH, Kwon SI, Ryu C, Park OK (2009) GDSL lipase-like 1 regulates systemic resistance associated with ethylene signaling in *Arabidopsis*. Plant J 58:235–245

Lan C, Liang S, Zhou X, Zhou G, Lu Q, Xia X, He Z (2010) Identification of genomic regions controlling adult-plant stripe rust resistance in Chinese landrace Pingyuan 50 through bulked segregant analysis. Phytopathology 100:313–318

Li ZQ, Zeng SM (2002) Wheat rust in China. China Agriculture Press, Beijing

Line RF, Qayoum A (1992) Virulence, aggressiveness, evolution, and distribution of races of *Puccinia striiformis* (the cause of stripe rust of wheat) in North America 1968–1987. US Department of Agriculture Technical Bulletin, p 74

Maccaferri M, Zhang J, Bulli P, Abate Z, Chao S, Cantu D, Bossolini E, Chen X, Pumphrey M, Dubcovsky J (2015) A genome-wide association study of resistance to stripe rust (*Puccinia striiformis* f. sp. *tritici*) in a worldwide collection of hexaploid spring wheat (*Triticum aestivum* L.). G3 5:449–465

Macer RCF (1966) The formal and monosomic genetic analysis of stripe rust (*Puccinia striiformis*) resistance in wheat. Hereditas 2:127–142

Mallard S, Gaudet D, Aldeia A, Abelard C, Besnard AL, Sourdille P, Dedryver F (2005) Genetic analysis of durable resistance to yellow rust in bread wheat. Theor Appl Genet 110:1401–1409

McIntosh RA, Wellings CW, Park RF (1995) Wheat rusts: an atlas of resistance genes. CSIRO Publications, East Melbourne, pp 20–26

McIntosh R, Mu J, Han D, Kang Z (2018) Wheat stripe rust resistance gene *Yr24/Yr26*: a retrospective review. Crop J 6:321–329

Meng L, Li HH, Zhang LY, Wang JK (2015) QTL IciMapping: integrated software for genetic linkage map construction and quantitative trait locus mapping in biparental populations. Crop J 3:269–283

Michelmore RW, Paran I, Kesseli RV (1991) Identification of markers linked to disease-resistance genes by bulked segregant analysis: a rapid method to detect markers in specific genomic regions by using segregating populations. Proc Natl Acad Sci USA 88:9828–9832

Moore JW, Herrera-Foessel S, Lan C, Schnippenkoetter W, Ayliffe M, Huerta-Espino J, Lillemo M, Viccars L, Milne R, Periyannan S, Kong X, Spielmeyer W, Talbot M, Bariana H, Patrick JW, Dodds P, Singh R, Lagudah E (2015) A recently evolved hexose transporter variant confers resistance to multiple pathogens in wheat. Nat Genet 47:1494–1498

Naruoka Y, Ando K, Bulli P, Muleta KT, Rynearson S, Pumphrey MO (2016) Identification and validation of SNP markers linked to the stripe rust resistance gene in wheat. Crop Sci 56:3055

Periyannan S, Milne RJ, Figueroa M, Lagudah ES, Dodds PN (2017) An overview of genetic rust resistance: from broad to specific mechanisms. PLoS Pathog 13:e1006380

Peterson RF, Campbell AB, Hannah AE (1948) A diagrammatic scale for estimating rust intensity on leaves and stems of cereals. Can J Res Sect C26:496–500

Qi LL, Echalier B, Chao S, Lazo GR, Butler GE, Anderson OD, Akhunov ED, Dvořák J, Linkiewicz AM, Ratnasiri A, Dubcovsky J, Bermudez-Kandianis CE, Greene RA, Kantety R, La Rota CM, Munkvold JD, Sorrells SF, Sorrells ME, Dilbirligi M, Sidhu D, Erayman M, Randhawa HS, Sandhu D, Bondareva SN, Gill KS, Mahmoud AA, Ma XF, Miftahudin, Gustafson JP, Conley EJ, Nduati V, Gonzalez-Hernandez JL, Anderson JA, Peng JH, Lapitan NL, Hossain KG, Kalavacharla V, Kianian SF, Pathan MS, Zhang DS, Nguyen HT, Choi DW, Fenton RD, Close TJ, McGuire PE, Qualset CO, Gill BS (2004) A chromosome bin map of 16,000 expressed sequence tag loci and distribution of genes among the three genomes of polyploid wheat. Genetics 168:701–712

Ramirez-Gonzalez RH, Uauy C, Caccamo M (2015) PolyMarker: a fast polyploid primer design pipeline. Bioinformatics 31:2038–2039

Rasheed A, Hao Y, Xia X, Khan A, Xu Y, Varshney RK, He Z (2017) Crop breeding chips and genotyping platforms: progress, challenges, and perspectives. Mol Plant 10:1047–1064

Ray DK, Ramankutty N, Mueller ND, West PC, Foley JA (2012) Recent patterns of crop yield growth and stagnation. Nat Commun 3:1293

Ren Y, He Z, Li J, Lillemo M, Wu L, Bai B, Lu Q, Zhu H, Zhou G, Du J, Lu Q, Xia X (2012) QTL mapping of adult-plant resistance to stripe rust in a population derived from common wheat cultivars Naxos and Shanghai 3/Catbird. Theor Appl Genet 125:1211–1221

Rosewarne GM, Herrera-Foessel SA, Singh RP, Huerta-Espino J, Lan CX, He ZH (2013) Quantitative trait loci of stripe rust resistance in wheat. Theor Appl Genet 126:2427–2449

Schlötterer C, Tobler R, Kofler R, Nolte V (2014) Sequencing pools of individuals—mining genome-wide polymorphism data without big funding. Nat Rev Genet 15:749–763

Sharma-Poudyal D, Chen XM, Wan AM, Zhan GM, Kang ZS, Cao SQ, Jin SL, Morgounov A, Akin B, Mert Z, Shah SJA, Bux H, Ashraf M, Sharma RC, Madariaga R, Puri KD, Wellings C, Xi KQ, Wanyera R, Manninger K, Ganzalez MI, Koyda M, Sanin S, Patzek LJ (2013) Virulence characterization of international collections of the wheat stripe rust pathogen, *Puccinia striiformis* f. sp. *tritici*. Plant Dis 97:379–386

Song WN, Ko L, Henry RJ (1994) Polymorphisms in the α-*amy1* gene of wild and cultivated barley revealed by the polymerase chain reaction. Theor Appl Genet 89:509–513

Stubbs RW (1985) Stripe rust. In: Roelfs AP, Bushnell WR (eds) The cereal rusts, vol II. Academic Press, New York, pp 61–101

Tang C, Xu Q, Zhao M, Wang X, Kang Z (2018) Understanding the lifestyles and pathogenicity mechanisms of obligate biotrophic fungi in wheat: the emerging genomics era. Crop J 6:60–67

Uauy C (2017) Wheat genomics comes of age. Curr Opin Plant Biol 36:142–148

Voorrips RE (2002) MapChart: software for the graphical presentation of linkage maps and QTLs. J Hered 93:77–78

Wan AM, Zhao ZH, Chen XM, He ZH, Jin SL, Jia QZ, Yao G, Yang JX, Wang BT, Li GB, Bi YQ, Yuan ZY (2004) Wheat stripe rust epidemic and virulence of *Puccinia striiformis* f. sp. *tritici* in China in 2002. Plant Dis 88:896–904

Wang JK (2009) Inclusive composite interval mapping of quantitative trait genes. Acta Agron Sin 35:239–245 **(in Chinese with English summary)**

Wang M, Wang S, Xia G (2015) From genome to gene: a new epoch for wheat research? Trends Plant Sci 20:380–387

Wang M, Wang S, Liang Z, Shi W, Gao C, Xia G (2018) From genetic stock to genome editing: gene exploitation in wheat. Trends Biotechnol 36:160–172

William HM, Singh RP, Huerta-Espino J, Palacios G, Suenaga K (2006) Characterization of genetic loci conferring adult plant resistance to leaf rust and stripe rust in spring wheat. Genome 49:977–990

Wu JH, Wang QL, Chen XM, Wang MJ, Mu JM, Lv XN, Huang LL, Han DJ, Kang ZS (2016) Stripe rust resistance in wheat breeding lines developed for central Shaanxi, an overwintering region for *Puccinia striiformis* f. sp. *tritici* in China. Can J Plant Pathol 38:317–324

Wu J, Wang Q, Liu S, Huang S, Mu J, Zeng Q, Huang L, Han D, Kang Z (2017) Saturation mapping of a major effect QTL for stripe rust resistance on wheat chromosome 2B in cultivar Napo 63 using SNP genotyping arrays. Front Plant Sci 8:653

Wu J, Huang S, Zeng Q, Liu S, Wang Q, Mu J, Yu S, Han D, Kang Z (2018a) Comparative genome-wide mapping versus extreme pool-genotyping and development of diagnostic SNP markers linked to QTL for adult plant resistance to stripe rust in common wheat. Theor Appl Genet 131:1777–1792

Wu J, Liu S, Wang Q, Zeng Q, Mu J, Huang S, Yu S, Han D, Kang Z (2018b) Rapid identification of an adult plant stripe rust resistance gene in hexaploid wheat by high-throughput SNP array genotyping of pooled extremes. Theor Appl Genet 131:43–58

Wu J, Wang Q, Xu L, Chen X, Li B, Mu J, Zeng Q, Huang L, Han D, Kang Z (2018c) Combining single nucleotide polymorphism genotyping array with bulked segregant analysis to map a gene controlling adult plant resistance to stripe rust in wheat line 03031-1-5 H62. Phytopathology 108:103–113

Wu J, Zeng Q, Wang Q, Liu S, Yu S, Mu J, Huang S, Sela H, Distelfeld A, Huang L, Han D, Kang Z (2018d) SNP-based pool genotyping and haplotype analysis accelerate fine-mapping of the wheat genomic region containing stripe rust resistance gene *Yr26*. Theor Appl Genet 131:1481–1496

Xu Y, Crouch JH (2008) Marker-assisted selection in plant breeding: from publications to practice. Crop Sci 48:391

Xu LS, Wang MN, Cheng P, Kang ZS, Hulbert SH, Chen XM (2013) Molecular mapping of *Yr53*, a new gene for stripe rust resistance in durum wheat accession PI 480148 and its transfer to common wheat. Theor Appl Genet 126:523–533

Xu Y, Li P, Zou C, Lu Y, Xie C, Zhang X, Prasanna BM, Olsen MS (2017) Enhancing genetic gain in the era of molecular breeding. J Exp Bot 68:2641–2666

Xue W, Xu X, Mu J, Wang Q, Wu J, Huang L, Kang Z, Han D (2014) Evaluation of stripe rust resistance and genes in Chinese elite wheat varieties. J Triticeae Crops 34:1054–1060 **(in Chinese with English summary)**

Zeng Q, Han D, Wang Q, Yuan F, Wu J, Zhang L, Wang X, Huang L, Chen X, Kang Z (2014) Stripe rust resistance and genes in Chinese wheat cultivars and breeding lines. Euphytica 196:271–284

Zeng QD, Shen C, Yuan FP, Wang QL, Wu JH, Xue WB, Zhan GM, Yao S, Chen W, Huang LL, Han DJ, Kang ZS (2015) The resistance evaluation of the *Yr* genes to the main prevalent pathotypes of *Puccinia striiformis* f. sp. *tritici* in China. Acta Phytopathol Sin 45:641–650 **(in Chinese with English summary)**

Zeng QD, Wu JH, Liu SJ, Chen XM, Yuan FP, Su PP, Wang QL, Huang S, Mu JM, Han DJ, Kang ZS (2018) Genome-wide mapping for stripe rust resistance loci in common wheat cultivar Qinnong 142. Plant Dis. https://doi.org/10.1094/pdis-05-18-0846-re

Zou C, Wang P, Xu Y (2016) Bulked sample analysis in genetics, genomics and crop improvement. Plant Biotechnol J 14:1941–1955